Eur. Phys. J. B **18**, 435–440 (2000)

THE EUROPEAN PHYSICAL JOURNAL B

EDP Sciences

The contribution of Gd and Mn neighbours to the Gd hyperfine field in $GdMn_6Ge_6$

M.T. Kelemen[1], P. Rösch[1], N. Kaplan[1,2], and E. Dormann[1,a]

[1] Physikalisches Institut, Universität Karlsruhe (TH), 76128 Karlsruhe, Germany
[2] Racah Institute of Physics, Hebrew University, Jerusalem, Israel

Received 31 May 2000 and Received in final form 26 September 2000

Abstract. With the help of ^{155,157}Gd NMR in $Gd_xY_{1-x}Mn_6Ge_6$ we derive the contribution of Gd and Mn neighbours to the hyperfine field at the rare earth site in the spiral spin phase of the intermetallic compound $GdMn_6Ge_6$. The substitution of Gd for Y atoms allows the determination of the separate contribution of remote Gd neighbours. The different temperature dependence of the hyperfine contributions of the Gd and Mn neighbours gives the possibility to estimate the transferred hyperfine field of Mn at the rare earth site both in magnitude and sign.

PACS. 76.60.Jx Effects of internal magnetic fields – 75.50.Gg Ferrimagnetics

1 Introduction

NMR is known to be a very sensitive method to derive hyperfine fields. In simple ferromagnetic intermetallic compounds and for zero external field, it gives accurate data on internal fields [1]. But also for more complicated compounds and especially for magnetically diluted pseudobinary compounds, it has been proven useful in estimating the strength and the distance dependence of the spin polarization of the conduction electrons [2]. In the present paper we describe some new experimental NMR results and associated model calculations related to the pseudoternary intermetallic compounds $Gd_xY_{1-x}Mn_6Ge_6$. The pure ($x = 1$) ternary crystal of this system represents one particular example of very many magnetically ordered intermetallic compounds containing both transition-metal and rare-earth components. The nature of the $4f - 3d$ exchange interaction in such systems is of crucial importance to the understanding of the magnetic properties exhibited. Because of the high degree of localization of the $4f$ local moments at the rare-earth site, a significant exchange interaction between the $4f$ and $3d$ moments is mediated indirectly *via* processes involving conduction-electron polarizations. The main aim of the present investigation is to delineate some of these polarizations.

The presently selected magnetic system is advantageous because of its relatively simple structure, with a single $4f$ and single $3d$ site, with the $4f$ moments residing in sites of high point symmetry.

The system $Gd_xY_{1-x}Mn_6Ge_6$ crystallize in the $HfFe_6Ge_6$-type structure (space group P6/mmm) [3,4]. It can be described as being built of alternate (001) layers containing Gd and Mn, respectively (Fig. 1). Whereas the Gd atoms form hexagonal planes (H), Mn atoms form Kagome nets (K) stacked along the c-axis with the sequence ...KHKKHK... [4]. Lattice constants vary linearly from $a = 5.2422$ Å and $c = 8.1843$ Å ($x = 1$) to $a = 5.2090$ Å and $c = 8.1110$ Å ($x = 0$). The preparation of the $Gd_xY_{1-x}Mn_6Ge_6$ powder samples has been

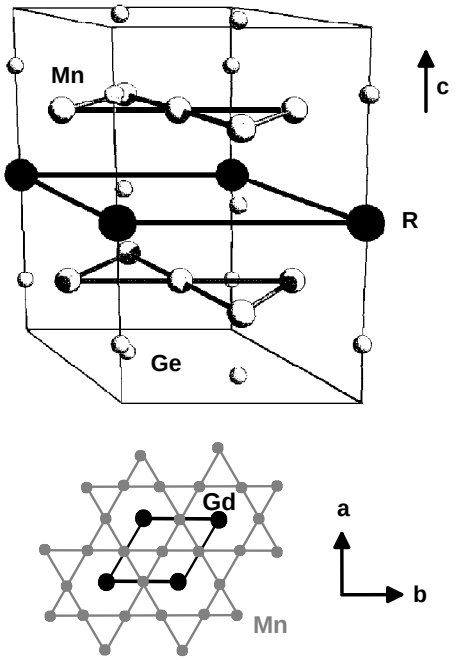

Fig. 1. Crystal structure of the $Gd_xY_{1-x}Mn_6Ge_6$ compounds and the Kagome net of the Mn atoms.

[a] e-mail: edo@piobelix.physik.uni-karlsruhe.de

described previously [4,5]. The pure ternary system and some pseudo-ternary Gd-Y compositions have been already the subject of numerous investigations in the past. Of immediate relevancy are studies related to the magnetic structure of the system (see for example references [6,5]), and in recent years also NMR and hyperfine field studies [7,8]. We will refer to the latter, as appropriate, also in the following sections.

The hyperfine field at a Gd-site in $GdMn_6Ge_6$ can be decomposed as follows

$$H_{\rm hf}({\rm Gd}) = H_{\rm CP} + H_{\rm S}({\rm Gd}) + H_{\rm N}({\rm Gd}) + H_{\rm T}({\rm Mn}). \quad (1)$$

$H_{\rm CP}$ represents the contribution due to the core polarization, and $H_{\rm S}$(Gd) stems from the polarization of the conduction electrons by the localized $4f$ moment at the same site [1,2]. $H_{\rm N}$(Gd) reflects the polarization caused by the $4f$ moments at all the other Gd sites in the crystal. Finally, $H_{\rm T}$(Mn) is the so called "transferred hyperfine field" contribution arising from the polarization of the conduction electrons by the $3d$ moments of the Mn sites throughout the crystal. As mentioned already, the last two contributions will be of primary interest in the study.

The paper is organized as follows: experimental NMR measurements on $Gd_xY_{1-x}Mn_6Ge_6$ samples, and the identification of the measured spectral lines with specific nuclei (and thus the determination of the associated hyperfine fields at relevant sites), are described in Section 2. The quantitative delineation of the various contributions to the hyperfine fields, and a discussion of the magnitudes and signs of these contributions, are presented in Section 3.

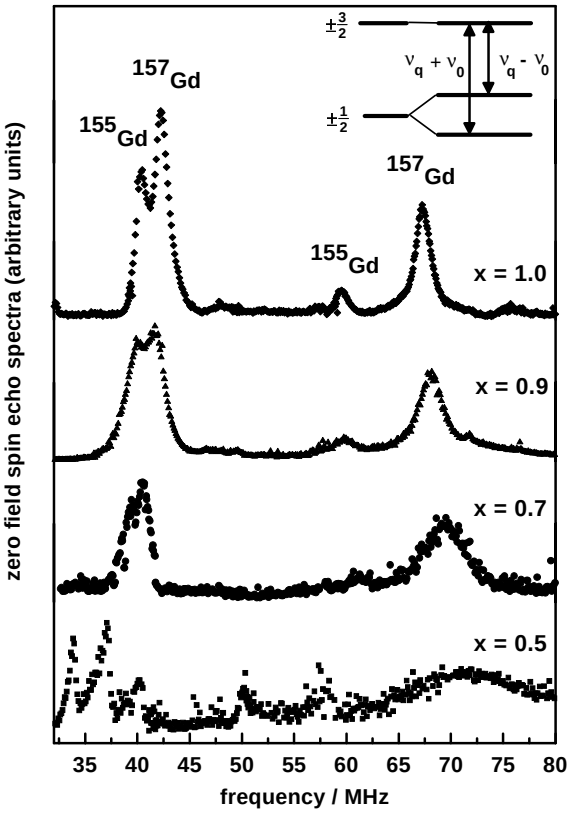

Fig. 2. ^{155,157}Gd spectra of several $Gd_xY_{1-x}Mn_6Ge_6$ compounds at 4.2 K in zero field. The inset shows the energy diagram for the case $\nu_0 \ll \nu_{\rm q}$ [11], and magnetic hyperfine field perpendicular to the main electric field gradient axis.

2 NMR spectra of $Gd_xY_{1-x}Mn_6Ge_6$

The NMR spectra were obtained using a commercial spectrometer (Bruker CXP200). Due to the enhancement of the rf field in the magnetically ordered $Gd_xY_{1-x}Mn_6Ge_6$ compounds, a tuned circuit was not required. Non-resonant coils with inner diameters of 5 mm, typical lengths of 10 mm and inductances of about 0.2 μH have been used. The spectra have been taken in zero field on powder samples sealed in glass tubes, using spin echoes. In general, the signal intensity was computed by integrating the Fourier transform of the second half of the acquired spin echo.

The upper dotted "trace" in Figure 2 shows the uncalibrated experimental spectrum of $GdMn_6Ge_6$ at 4.2 K in zero field. This one, as well as the other $Gd_xY_{1-x}Mn_6Ge_6$ spectra shown, were measured using an rf pulse sequence with pulses of 2 μs and 3 μs, separated by an interval of 15 μs. For each curve, the signal amplitude was optimized with respect to transmitter power. The power required was around 0.2 W for all analysed compounds, corresponding to a H_1 amplitude of about 0.5 Oe.

Altogether four NMR transitions between 33 MHz and 80 MHz are observed. As will be outlined presently, these could be identified as transitions of the ^{155}Gd and ^{157}Gd isotopes, taking into account that both have a spin of 3/2 [9].

The zero-field ^{155,157}Gd spectra appear to be dominated by quadrupolar interactions. However, analysis of the spectra is complicated by the fact that the nuclear Zeeman interaction is not negligible. For convenience, we will use the conventional nomenclature with ν_0 representing the nuclear Zeeman frequency at zero external field, and $\nu_{\rm q}$ representing the nuclear quadrupolar frequency [10]. We note that the condition $\nu_0 \ll \nu_{\rm q}$ is not strictly fulfilled as $\nu_{\rm q}/\nu_0 \leq 5$, and thus a simple perturbation approach to the problem is not appropriate. Diagonalizing the sum-hamiltonian describing both the quadrupolar and the Zeeman interactions (transformed into the eigensystem of the electric field gradient tensor), one finds the two relevant transition frequencies ν_1 and ν_2 [8] which are given by

$$\begin{aligned}\nu_1 &= \frac{3}{4}\sqrt{4\nu_0^2 + 2\nu_0\nu_{\rm q} + \nu_{\rm q}^2} \\ &\quad + \frac{1}{4}\sqrt{4\nu_0^2 - 2\nu_0\nu_{\rm q} + \nu_{\rm q}^2} + \frac{1}{2}\nu_0 \\ \nu_2 &= \frac{1}{4}\sqrt{4\nu_0^2 + 2\nu_0\nu_{\rm q} + \nu_{\rm q}^2} \\ &\quad + \frac{3}{4}\sqrt{4\nu_0^2 - 2\nu_0\nu_{\rm q} + \nu_{\rm q}^2} - \frac{1}{2}\nu_0 \end{aligned} \quad (2)$$

The inset in Figure 2 shows these transitions in the limit $\nu_q i \gg \nu_0$ taking $\theta = 90°$. This angle describes the direction of the hyperfine field with respect to the main axis of the field gradient, assuming the *c*-axis as the preferred direction because of the axial symmetry of the Gd sites. The apparent "degeneracy" of the $\pm 3/2$ energy levels plotted in the inset is merely a consequence of $\theta = 90°$ in combination with the above limiting condition on ν_0.

Equations (2) were solved for ν_q and ν_0, using the values of $^{155}\nu_1$, $^{157}\nu_1$, $^{155}\nu_2$ and $^{157}\nu_2$ shown for 4.2 K in Figure 2. From these resonance positions we obtain a quadrupole frequency of $\nu_q = 46.9$ MHz (49.7 MHz) and a Zeeman frequency of $\nu_0 = 9.91$ MHz (13.1 MHz) for the isotope ^{155}Gd (^{157}Gd). The average ratio $^{157}\nu_0/^{155}\nu_0 = 1.33$ is in good agreement to the value $^{157}\gamma/^{155}\gamma = 1.31$ reported for $GdAl_2$ [12]. The ratio $^{157}\nu_q/^{155}\nu_q = 1.059$ differs by less than one percent from the published [13] result of $^{157}Q/^{155}Q = 1.065$. The above ratio-tests add credence to the assumption that the 4 transitions shown in Figure 2 are indeed the only ones in the spectral range of 35-80 MHz to be associated with the two Gd isotopes, thus confirming that the hyperfine field and with this also the local magnetisation are in the plane perpendicular to the *c* axis.

The zero field spectra of the compounds $Gd_xY_{1-x}Mn_6Ge_6$ show essentially no structural change with decreasing Gd concentration down to $x = 0.7$ (Fig. 2). This implies that the local magnetisation remains in a plane perpendicular to the *c*-axis for all of these compounds. The Zeeman frequency of both isotopes increases with decreasing concentration, the quadrupole frequency shows a little decrease (Tab. 1). The low-frequency transitions of both isotopes approach each other whereas the transitions at the higher frequency broaden.

A severe line-broadening is observed for the compound with $x = 0.5$, and additional transitions appear. The new transitions, not predicted by equation (2), indicate that the assumption of a hyperfine field lying perpendicular to the *c*-axis is no longer strictly valid at this concentration. We could still discern some of the original transitions, and extrapolated signals have been used to analyse and derive some approximate values for the hyperfine and quadrupole frequencies also for $x = 0.5$, assuming $\theta = 90°$.

3 Delineation of the Gd hyperfine field

The hyperfine field values at the Gd nuclear site are obtained by substracting the Lorentz field from the effective fields $2\pi\nu_0/\gamma$, using the frequencies listed in Table 1 (second column). No demagnetization field correction is needed because of the vanishing macroscopic magnetization. The last column in Table 1 lists the results for each concentration and isotope in field units.

For further analysis, we must determine the sign of the Gd hyperfine field, perhaps better defined as the direction of the hyperfine field (parallel or antiparallel) with respect to the total resultant unit-cell magnetization. In many cases this sign is determined from the frequency shift in external field, but for Gd in the present compounds this is not possible due to the nonlinear relation in equation (2). Thus, we shall use a simple reasoning based on reported relevant attributes. It was concluded previously that each Mn atom carry approximately $2\mu_B$, and the six Mn atoms in the ferrimagnetic unit-cell point in parallel, with a resultant moment of approximately $12\mu_B$ [6,5,8,14]. The Gd atom in metallic systems carries always a well localized moment of $7\mu_B$. We also note that magnetization measurements in the ferrimagnetic phase of the system always yield a resultant total moment of approximately $\mu_S = (12 - 7x)\mu_B$ per unit-cell [14]. The only way to reconcile all these facts is by concluding that the Gd moment points antiparallel to the direction of the vector-sum of the 6 neigboring Mn moments, and therefore also antiparallel to the direction of the resultant total moment of the unit-cell, $\bar{\mu}_S$.

Table 1. Zeeman-, quadrupole frequencies and hyperfine fields of ^{155,157}Gd.

x	$^{155}\nu_0$ / MHz	$^{155}\nu_q$ / MHz	H_{hf}^{155} / kOe
1.0	9.91	46.9	74.6
0.9	10.4	46.5	78.2
0.8	11.1	45.9	83.4
0.7	11.1	45.8	-
0.5	-	-	-
x	$^{157}\nu_0$ / MHz	$^{157}\nu_q$ / MHz	H_{hf}^{157} / kOe
1.0	13.1	49.7	75.7
0.9	13.7	49.1	79.3
0.8	14.6	48.3	84.0
0.7	15.7	47.5	90.6
0.5	17.8	46.0	94.0

We now make use of the fact that by far the dominant contribution to the hyperfine field in Gd is usually the negative core polarization term H_{CP} of equation (1) [1], and here "negative" means pointing antiparallel to the direction of the Gd moment. The resulting – usually smaller – total hyperfine field at the Gd site H_{hf}(Gd) of equation (1) will also point antiparallel to the Gd moment, and therefore parallel to the Mn magnetization in the unit-cell. We define this direction in the unit-cell as "positive".

The magnitude of the Gd core polarisation in our present system is estimated as 332 kOe [1,2] and in view of the above sign determinations we can write also

$$H_{CP} = +332 \text{ kOe}. \quad (3)$$

We wish to examine now which of the possible different statistical Gd configurations is reflected in the observed spectra for $x < 1.0$. To characterise the contributions of the Gd neighbours to the hyperfine field, it is important to calibrate the relative Gd signal intensities observed in the different compounds. This can be elegantly accomplished by the help of the Ge(2) spectra. For this site the effective field does not change with varying Gd concentrations [14], depending only on the transfered hyperfine field contributions from Mn moments. That means that the ^{73}Ge NMR

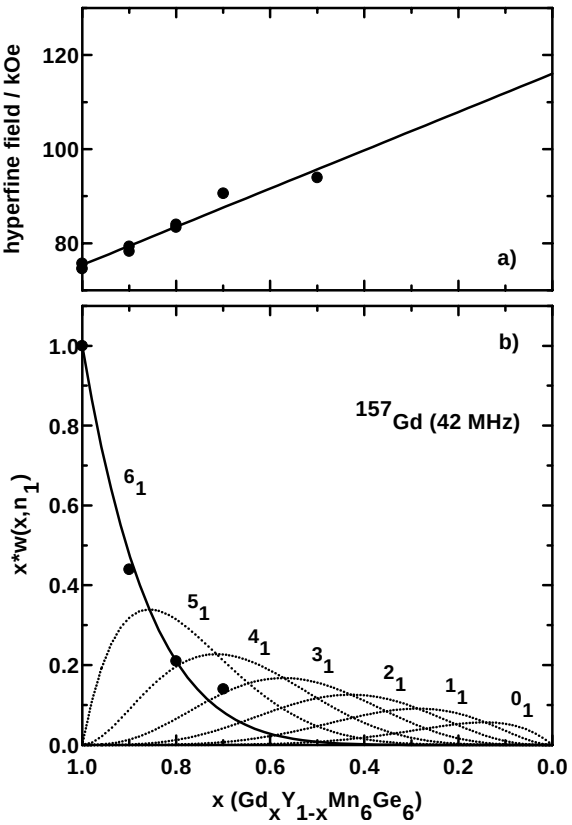

Fig. 3. a) Concentration dependence of the hyperfine fields of ^{155,157}Gd ($T = 4.2$ K). b) Normalized signal amplitudes of the ^{157}Gd resonance at 42 MHz for different concentrations (points). The solid and broken curves labeled by n_1 show the theoretical dependencies for different Gd occupation values n in the first shell, according to equation (4).

signal, for example at 27 MHz ($x = 1.0$), should be equal to the respective signal in each of the other ($x \neq 1.0$) compounds, and its amplitude I_x(Ge) for each sample can be used as a calibration standard. Accordingly, values of the intensity ratio $I_x(\mathrm{Gd})/I_x(\mathrm{Ge})$ for all the samples provide a properly normalised Gd signal intensity as function of x, shown as filled points in Figure 3b. The echo intensities of all the measured signals were first extrapolated to $\tau = 0$ to correct for echo decays.

To interpret the concentration dependence of the Gd hyperfine field, we consider the possible statistical occupations of neighbored Gd places. For a Gd concentration x and a neighbor shell i with N_i sites, the probability for the occurrence of n_i Gd ions in the ith shell is [15]

$$w(x, n_i) = \frac{N_i!}{(N_i - n_i)! n_i!}(1-x)^{N_i - n_i} x^{n_i} \qquad (4)$$

with

$$\begin{aligned} N_1 &= 6\ ,\ R_1 = a \\ N_2 &= 2\ ,\ R_2 = c \\ N_3 &= 6\ ,\ R_3 = \sqrt{3}a. \end{aligned} \qquad (5)$$

The curves in the lower part of Figure 3 show the dependence of the intensity ($x \times w(x, n_1)$) for different occupations n_1 of the nearest Gd neighbour shell on the Gd concentration x. The measured intensities are in very good agreement with the curve for a completely filled nearest neighbour shell. Therefore the measured hyperfine field at the Gd nucleus can be written as

$$\begin{aligned} H_{\mathrm{hf}}(\mathrm{Gd}) = H_{\mathrm{CP}} + H_{\mathrm{S}}(\mathrm{Gd}) + 6H_{\mathrm{nn}}(\mathrm{Gd}) \\ + xH_{\mathrm{RN}}(\mathrm{Gd}) + H_{\mathrm{T}}(\mathrm{Mn}) \end{aligned} \qquad (6)$$

whereby H_{nn}(Gd) is describing the part of the hyperfine field transferred from a single Gd nearest neighbour. Figure 3 explains thus also the rapid decrease of the Gd signal intensity with decreasing Gd concentration, assuming only the 6_1 configuration contribute to the observed signal. The absence of resolved signals from n_1 configurations with $n \leq 5$ is probably a manifestation of the severely disturbed symmetry of the EFG in such configurations.

Equation (6) includes also a term describing the linear dependence between the hyperfine field and the Gd concentration, shown in the upper part of Figure 3. In the way written, the parameter H_{RN} represent the contribution to the hyperfine field in a sample with $x = 1.0$ arising from all the N_i Gd moments with $i \geq 2$, *i.e* all the remaining Gd moments except those in the nearest neighbour shell. Since the sign of the hyperfine field was already established as positive, the slope of the curve in Figure 3a yields directly

$$H_{\mathrm{RN}}(\mathrm{Gd}) = -40.65\ \mathrm{kOe} \qquad (7)$$

Substracting the core polarization contribution, the hyperfine field derived from the intercept at $x = 0$ yield the summed contributions of the nearest Gd neighbours $6H_{\mathrm{nn}}$(Gd), the term H_{S}(Gd), and the transferred hyperfine field contribution of Mn moments.

We turn now to the H_{T}(Mn) term. The temperature dependence of the Gd hyperfine field in Figure 4 gives the possibility to estimate the transferred hyperfine field of Mn. Only an outline of the analysis is currently presented, and for some of the theoretical details, the reader is referred to references [8,17]. The local magnetisation of Gd can be described using a Brillouin function with a spin of 7/2. Assuming the same functional form also for the total Gd hyperfine field, we can write

$$\frac{\nu_0(T)}{\nu_0(4\,\mathrm{K})} = B_{7/2}\left(\frac{g\mu_{\mathrm{B}} H_{\mathrm{eff}}}{k_{\mathrm{B}} T}\right) \cdot \qquad (8)$$

We can try now to fit the parameter in the right side of equation (8) to the experimental points from Figure 4. Using only values for $T \leq 140$ K, we obtain the fitted curve M_1, and an effective exchange coupling constant of

$$A_{\mathrm{eff}}^{\mathrm{Gd}}/k_{\mathrm{B}} = 40.8\ \mathrm{K} \qquad (9)$$

is derived for $GdMn_6Ge_6$. The predicted critical temperature, lying near the phase transition between ferrimagnetic and flat spiral spin structure [16], is around 215 K.

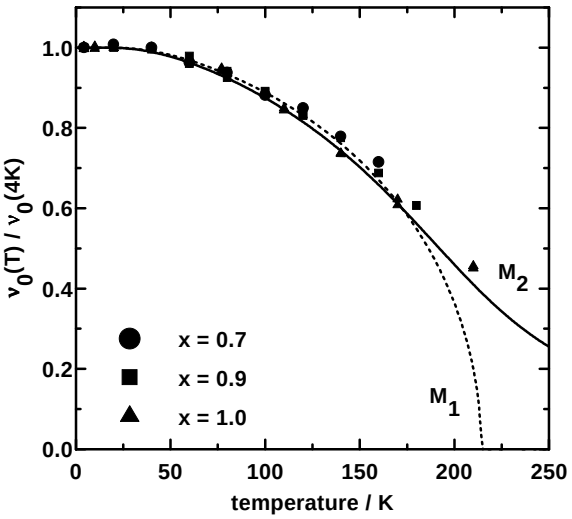

Fig. 4. Temperature dependence of the ^{155,157}Gd Zeeman frequencies for different $Gd_xY_{1-x}Mn_6Ge_6$ compounds. The solid and broken lines are fits based on a Brillouin function for $S = 7/2$. M_1: fit without H_T(Mn) contribution. M_2: fit with H_T(Mn) contribution.

The coupling strength is in good agreement with the ferromagnetic coupling constant obtained earlier [14] for the Gd sublattices using mean-field model calculations.

The curve M_1, however, does not account well for the observations at $T \geq 150$ K, neither for the pure ternary system [8] nor for the mixed Gd-Y samples shown in Figure 4. As is evident from the presented data, a significant additional contribution to the hyperfine field at the Gd site is unraveled as we get nearer to the predicted transition point around 215 K. As equation (8) does not include the thermodynamics of the Mn contributions to the hyperfine field, it is reasonable to conclude that the apparent extra contribution at higher temperature reflects the non-vanishing magnetization of the Mn sublattice even close to the transition temperature. Even before any modeling, we can conclude intuitively that this contribution is positive with respect to the "rest" of the Gd hyperfine field. A more quantitative treatment related to the pure ternary system was discussed recently [8,17]. A mean-field model calculation was used, which included, in addition to the field determined by the thermodynamics of the Gd sublattice, also a colinear Mn-induced term. The latter was scaled with the sublattice magnetization of the Mn [14,17]. The fitted model calculation is plotted as curve M_2 in Figure 4, yielding for the Mn transferred hyperfine field a value of

$$H_T(\text{Mn}) = +33 \text{ kOe}. \tag{10}$$

Finally, we can collect now all the known terms in equation (6) to find

$$H_S(\text{Gd}) + 6H_{nn}(\text{Gd}) = -249 \text{ kOe} \tag{11}$$

and this concludes our analysis of the Gd hyperfine field in the $GdMn_6Ge_6$ system. For convenience, we list again in Table 2 the numerical values for the relevant terms discussed in this section.

Table 2. Delineation of the various contributions to the hyperfine fields at ^{155,157}Gd.

Term	Value/kOe
H_{hf}(Gd)	+ 75.1
H_{CP}	+ 332
H_{RN}	−40.65
H_T(Mn)	+ 33
H_S(Gd) + $6H_{nn}$(Gd)	−249

4 Summary and concluding remarks

We have shown that with the NMR of ^{155,157}Gd in $Gd_xY_{1-x}Mn_6Ge_6$ only the configurations with 6 nearest Gd neighbours contribute to the H_N(Gd) term in our experimentaly resolved Gd NMR spectra, independent of the concentration in the range $0.5 \leq x \leq 1.0$. From these spectra, the value of the total hyperfine field at the rare-earth site, H_{hf}(Gd), was determined for the pure ternary compound $GdMn_6Ge_6$. The substitution of Gd atoms by Y atoms allows the determination of the separate contribution of remote Gd neighbours [H_{RN}(Gd)] to the H_N(Gd) term. The different thermodynamic behaviour of the Gd and Mn sublattice magnetizations enabled an estimate of the transferred hyperfine field of Mn at the rare earth site in magnitude and sign. From the presence of a significant Gd hyperfine field around 220 K we may also deduce the existence of some Gd magnetization at this temperatures. This probably indicates that within the ferrimagnetic phase above 215 K, Gd moments are magnetized through the transferred conduction electron polarization of the Mn sublattice. If that is indeed case, then the existence of the low temperature flat spiral spin structure in $GdMn_6Ge_6$ could be linked with spontaneous ordering of the Gd moments caused by effective Gd-Gd exchange interactions.

One final remark before concluding. It is intuitively obvious in the present context that H_{nn}(Gd) is related to the indirect exchange interaction J_{ff} between neigboring Gd moments, whereas H_T(Mn) is related to the indirect exchange interaction J_{4f-3d} between Gd and Mn. It is therefore somewhat disapointing that while we could determine the experimental value of H_T(Mn), only the algebraic sum of $6H_{nn}$(Gd) + H_S(Gd) could be determined presently. Since H_S has no direct relevancy to indirect exchange interactions, a further separation of the two terms remains a deserving goal. In principle one could achieve such separation by measuring the Gd NMR signal in $Gd_xY_{1-x}Mn_6Ge_6$ in the limit of very small x. With saturating external field and sufficiently low temperature, the Gd ($n_1 = 0$) frequency will reflect only the H_T(Mn) and H_S(Gd) contributions, and a complete separation is possible with the known value of H_T.

This work was financially supported by the Deutsche Forschungsgemeinschaft. We thank K.H.J. Buschow for the samples.

References

1. E. Dormann, *NMR in intermetallic compounds*, in *Handbook on the Physics and Chemistry of Rare Earths*, edited by K.A. Gscheidner Jr, LeRoy Eyring (North-Holland, 1991), Vol. 14, p. 63
2. E. Dormann, M. Huck, K.H.J. Buschow, J. Magn. Magn. Mat. **4**, 47 (1977).
3. G. Venturini, R. Welter, B. Malaman, J. Alloys Comp. **185**, 99 (1992).
4. J.H.V.J. Brabers, V.H.M. Duijn, F.R. de Boer, K.H.J. Buschow, J. Alloys Comp. **198**, 127 (1993).
5. F.M. Mulder, R.C. Thiel, J.H.V.J. Brabers, F.R. de Boer, K.H.J. Buschow, J. Alloys Comp. **190**, L29 (1993).
6. G. Venturini, R. Welter, B. Malaman, E. Ressouche, J. Alloys Comp. **200**, 51 (1993).
7. P. Rösch, J. Weizenecker, M.T. Kelemen, J. Ruf, C. Zobel, E. Dormann, J. Magn. Magn. Mat. **177-181**, 1071 (1998).
8. P. Rösch, M.T. Kelemen, E. Dormann, G. Tomka, P.C. Riedi, J. Phys. Cond. Matt. **12**, 1065 (2000).
9. For the convenience of the reader, we repeat now some of the arguments already presented in reference [8].
10. T.P. Das, E.L. Hahn, in *Nuclear Quadrupole Resonance Spectroscopy*, Solid State Physics, Suppl. 1, edited by F. Seitz, D. Turnbull (Acad. Press, 1958).
11. G.C. Carter, L.H. Bennett, D.J. Kahan, *Metallic shifts in NMR,* Progress in Materials Science, Part I, Vol. 20, edited by B. Chalmers, J.W. Christian, T.B. Massalski (Pergamon, Oxford, 1977), p. 79.
12. E. Dormann, U. Dressel, H. Kropp, K.H.J. Buschow, J. Magn. Magn. Mat. **45**, 207 (1984).
13. P.J. Unsworth, J. Phys. B **2**, 122 (1969).
14. M.T. Kelemen, P. Rösch, E. Dormann, K.H.J. Buschow, J. Magn. Magn. Mat. **188**, 195 (1998).
15. E. Dormann, K.H.J. Buschow, K.N.R. Taylor, G. Brown, M.A.A. Issa, J. Phys. F **3**, 220 (1973).
16. P. Rösch, M.T. Kelemen, B. Pilawa, E. Dormann, K.H.J. Buschow, J. Magn. Magn. Mat. **164**, 175 (1996).
17. M. Kelemen, Ph.D. thesis, Universität Karlsruhe, 1999 and Cuvillier Verlag, Göttingen, 1999.